Applied Catalysis B: Environmental 84 (2008) 162–169

Contents lists available at ScienceDirect

Applied Catalysis B: Environmental

journal homepage: www.elsevier.com/locate/apcatb

Catalytic activity and aging phenomena of three-way catalysts in a compressed natural gas/gasoline powered passenger car

Alexander Winkler [a,*], Panayotis Dimopoulos [a], Roland Hauert [b], Christian Bach [a], Myriam Aguirre [c]

[a] Empa, Swiss Federal Laboratories for Materials Testing and Research, Laboratory for Internal Combustion Engines, Ueberlandstrasse 129, CH-8600 Duebendorf, Switzerland
[b] Empa, Swiss Federal Laboratories for Materials Testing and Research, Laboratory for Nanoscale Materials Science, Ueberlandstrasse 129, CH-8600 Duebendorf, Switzerland
[c] Empa, Swiss Federal Laboratories for Materials Testing and Research, Laboratory for Solid State Chemistry and Analyses, Ueberlandstrasse 129, CH-8600 Duebendorf, Switzerland

ARTICLE INFO

Article history:
Received 31 January 2008
Received in revised form 18 March 2008
Accepted 21 March 2008
Available online 29 March 2008

Keywords:
Three-way catalyst
Catalyst aging
Methane oxidation
Compressed natural gas
XPS
SEM
BET

ABSTRACT

The catalytic activity of the pre(p)- and the underfloor(u) three-way catalysts (TWCs), of a bifuel passenger car (compressed natural gas (CNG), gasoline), has been examined at a series of mileage milestones. Over a rather short lifetime of 35,000 km, a significant increase of the unburned total hydrocarbons (THC) has been determined during CNG operation. No comparable THC increase in the exhaust was found during gasoline operation. The THC increase was detected at exhaust temperatures well over 633 K, excluding methane specific light-off deterioration. Possible explanations for this fuel selective behaviour could be identified by the application of different surface techniques. XPS analysis hints to the formation of a metallic Pd layer formed over the catalytically active PdO core, probably having the highest impact on the decreased methane oxidation during CNG operation. Typical lubricating oil based contaminants like P, Ca, and Mg, have been detected on the catalysts' surface as well.

1. Introduction

Stringently regulated automotive exhaust gas emissions according to standards like Euro 4 (in effect since January 1, 2005) or Euro 5 (September 1, 2009), require the employment of complex strategies for emission reduction. The three-way catalyst (TWC) plays a key role in the abatement of hazardous exhaust gas components of spark ignition engines [1,2].

Although TWCs have proven to be efficient even after high mileage, increasingly stringent emission standards, high precious metal (PM) costs and new fuel concepts (e.g. CNG; over 90 vol.% methane [3]) raised new issues. Compressed natural gas (CNG) fuelled vehicles have, at least in Europe, increasing popularity. CNG has high availability, low price and, in comparison to gasoline, it produces smaller quantities of carbon dioxide and other pollutants per unit of power generated [4]. On the other hand, methane (CH_4) is a much more potent greenhouse gas than carbon dioxide, and unburned CH_4 is, in contrast to gasoline powered vehicles, the major hydrocarbon exhaust gas component in CNG vehicles [5]. This poses a problem with regard to fulfilling HC emission standards, since methane is also one of the most difficult hydrocarbons to catalytically oxidize. In addition, the exhaust gas temperature of CNG engines is lower in comparison to gasoline vehicles [4,6,7], thus impeding the catalytic conversion even further. The results published by Takigawa et al. [8] underline the problem. It was shown that the catalyst HC oxidation activity is selectively lower for CH_4 in comparison to all other alkanes analyzed.

In this paper we tracked the evolution of the emissions of a commercially available bifuel (CNG/gasoline) passenger car. At each mileage milestone the emissions of the vehicle have been measured, comparing the CNG and gasoline operation each time. The vehicle catalysts were analyzed, employing XPS, SEM and BET, and compared with new and oven aged catalysts of the same type. On the basis of the findings an analysis of reasons for the CNG-selective loss of catalytic activity for methane is provided.

* Corresponding author. Tel.: +41 44 823 4333; fax: +41 44 823 4044.
E-mail address: alexander.winkler@empa.ch (A. Winkler).

Abbreviations: BET, Brunauer, Emmett, Teller; CADC, Common Artemis Driving Cycle; CLD, Chemical Luminescence Detector; CNG, Compressed Natural Gas; ECE, Economic Commission for Europe (driving cycle); EUDC, Extra Urban Driving Cycle; FID, Flame Ionisation Detector; GC, Gas Chromatograph; NDIR, Non-Dispersive InfraRed (analyzer); NEDC, New European Driving Cycle; NMHC, Non Methane HydroCarbons; PM, Precious Metal; RSF, Relative Sensitivity Factor; SEM, Scanning Electron Microscopy; SSA, Specific Surface Area; THC, Total HydroCarbons; p-TWC, Pre Three-Way Catalyst; u-TWC, Underfloor Three-Way Catalyst; WS, Washcoat; XPS, X-ray Photoelectron Spectroscopy.

0926-3373/$ – see front matter © 2008 Elsevier B.V. All rights reserved.
doi:10.1016/j.apcatb.2008.03.013

2. Experimental

The used vehicle was a commercially available serial production bifuel passenger car from a European OEM. It is one of the best sold bifuel vehicles in the European market. Vehicle aging was carried out on the road, during every day use. Vehicle operation monitoring revealed approximately 90% CNG operation, and only 10% gasoline operation. The fuel used was the regular Swiss CNG available on the gas stations comparable to H-gas quality. The driving patterns have been almost balanced among urban, extra urban and highway driving (35,000 km corresponding to roughly 800 operating hours), extra urban and highway occurred more often. Initial, final as well as intermediate measurements have been performed with standard fuels of our laboratory corresponding to the Swiss standards. During natural gas operation on the dynamometer, we used G20 (100% methane) as a fuel.

The exhaust gas aftertreatment system comprised of a small pre-TWC (p-TWC), installed in close vicinity to the engine, and the underfloor-TWC (u-TWC), further downstream in the exhaust gas path. Both catalytic converters consisted of a cordierite monolith carrier with applied washcoat. According to manufacturers' instruction, the total PM content of the p-TWC was 75 g/ft^3. It contained Pt, Pd and Rh in different concentrations with the Pd content being the highest. The PM content of the u-TWC amounted to 250 g/ft^3. Both the vehicle aged p-TWC and u-TWC has been analyzed. For comparison new as well as oven aged (muffle furnace, 1173, 1373 K/3 h) catalysts of the same type have also been analyzed. All samples were taken from the catalyst centre about 2 cm away from the catalyst intake. For XPS and SEM analysis rectangular pieces about 2 mm × 5 mm × 20 mm in size have been extracted.

The *exhaust gas analysis* included the limited pollutants carbon monoxide (CO), total hydrocarbons (THC), non-methane hydrocarbons (NMHC), nitrogen oxides (NO_x) and carbon dioxide (CO_2). The measurements were performed on a 1-roller chassis dynamometer equipped with exhaust gas analyzers for CO (NDIR), THC (FID) and NO_x (CLD) according to European Directive 70/220/EC [9]. A CH_4 response factor of 1.04 was determined for the propane-calibrated THC analyzer (FID). In addition, CH_4 emissions were measured with a methane-calibrated GC–FID. Fig. 1 shows a schematic of the experimental setup.

The reported emission results are mainly based on measurements during the New European Driving Cycle (NEDC), used for type approval purposes and the more real world driving conditions representing Common Artemis Driving Cycle (CADC) (Fig. 2). The NEDC consists of two parts, the urban ECE (duration: 780 s, maximum speed: 50 km/h), and the extra-urban EUDC (duration: 400 s, maximum speed: 120 km/h). The ECE starts with a cold engine. The car available automatically switches to gasoline for the cold start (a strategy followed by almost all European bifuel cars up to now) and switches back to CNG after a threshold temperature is reached. Therefore, we did not use ECE emissions for further analysis.

The CADC is considered to be the most realistic driving cycle [10]. It is composed of an urban (duration: 920 s, maximum speed: 58 km/h), an extra urban road (duration: 980 s, maximum speed: 112 km/h), and a highway part (duration: 735 s, maximum speed: 150 km/h), Fig. 2. The start occurs with warmed up engine and so emission results between pure CNG and pure gasoline operation can be compared throughout the entire CADC as well as among each of the parts comprising it. Fig. 2 also includes the temperature profile at the entrance of the u-TWC for both cycles.

XPS spectra were acquired on a Physical Electronics (PHI) Quantum 2000 photoelectron spectrometer using monochromated AlKα radiation and a hemispherical capacitor electron-energy analyzer equipped with a channel plate and a position-sensitive detector. The electron take-off angle was 45° and the analyzer was operated in the constant pass energy mode (117.4 eV, calibrated to a total analyzer energy resolution of 1.62 eV for Ag 3d electrons) for all measurements. The beam diameter was typically 100 μm, thus allowing analyzing only the washcoat covered monolith channel. Special care was taken to avoid the uncovered wall fractures during analysis.

Sputtering was performed with Ar^+, the acceleration energy was 4 kV. Thirty-six seconds of sputtering resulted in a depth of about 10 nm.

Quantitative analysis required signal deconvolution which was performed employing the nonlinear least square curve fitting software "Spectral Data Processor V4.3" [11]. PHI sensitivity factors were used for the calculation. The C 1s signal position at 284.8 eV binding energy (BE) was used as an internal standard for calibration of the XP-signal positions. In case of sputtered samples, the Ar 2s signal position at 320.0 eV BE was used for calibration.

SEM images were recorded on a high resolution Hitachi S-4800 SEM employing an acceleration voltage of 10 kV, a work distance of 8 mm and an upper secondary electron detector. The magnification of all images was ×50,000. The rectangular p- and u-TWC samples were glued to the sample holder using a conductive carbon

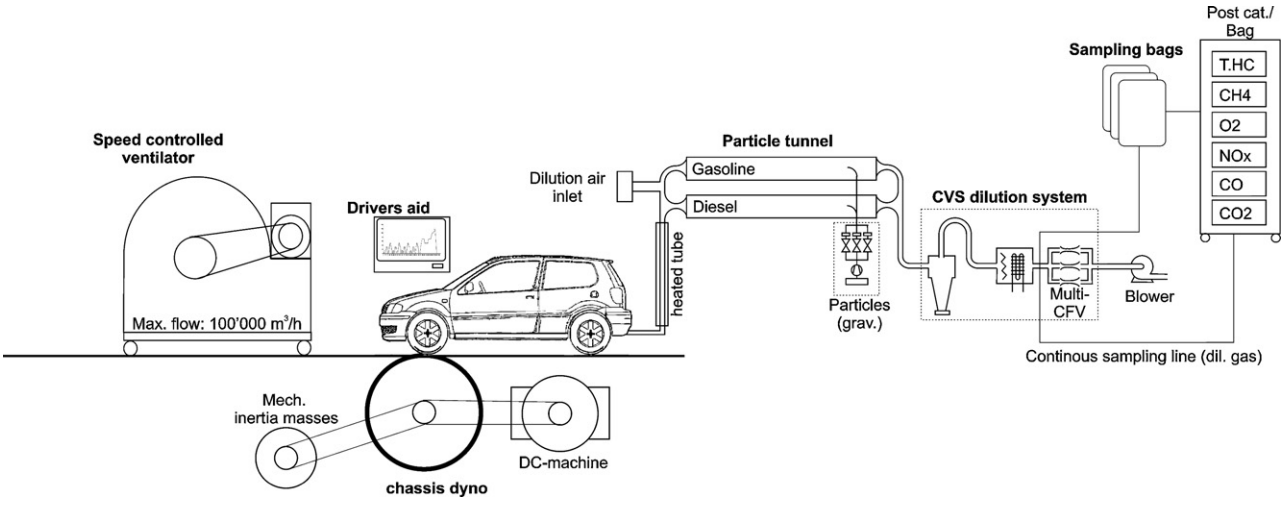

Fig. 1. Schematic of the chassis dynamometer as well as the exhaust analyzing equipment.

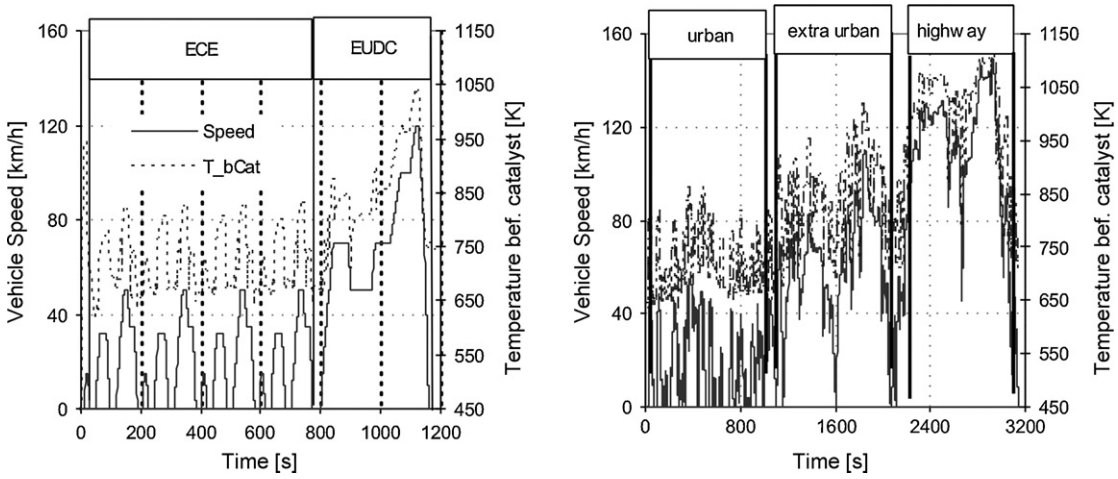

Fig. 2. Velocity-time profiles of the NEDC (left) and the CADC (right) driving cycles. The dotted line in both figures is the corresponding exhaust gas temperature measured at the u-TWC entrance.

solution and sputter coated with an 8 nm layer of platinum. The film thickness was controlled via a quartz microbalance.

Dynamic single point *BET* analysis was performed on a Chembet-3000 from Quantachrome Instruments, employing a gas mixture containing 30.21 mol% nitrogen in helium. The p- and u-TWC samples were cut from the respective monoliths, ground in an agate mortar and, prior to analysis, baked out for 2 h at 473 K under a nitrogen flow.

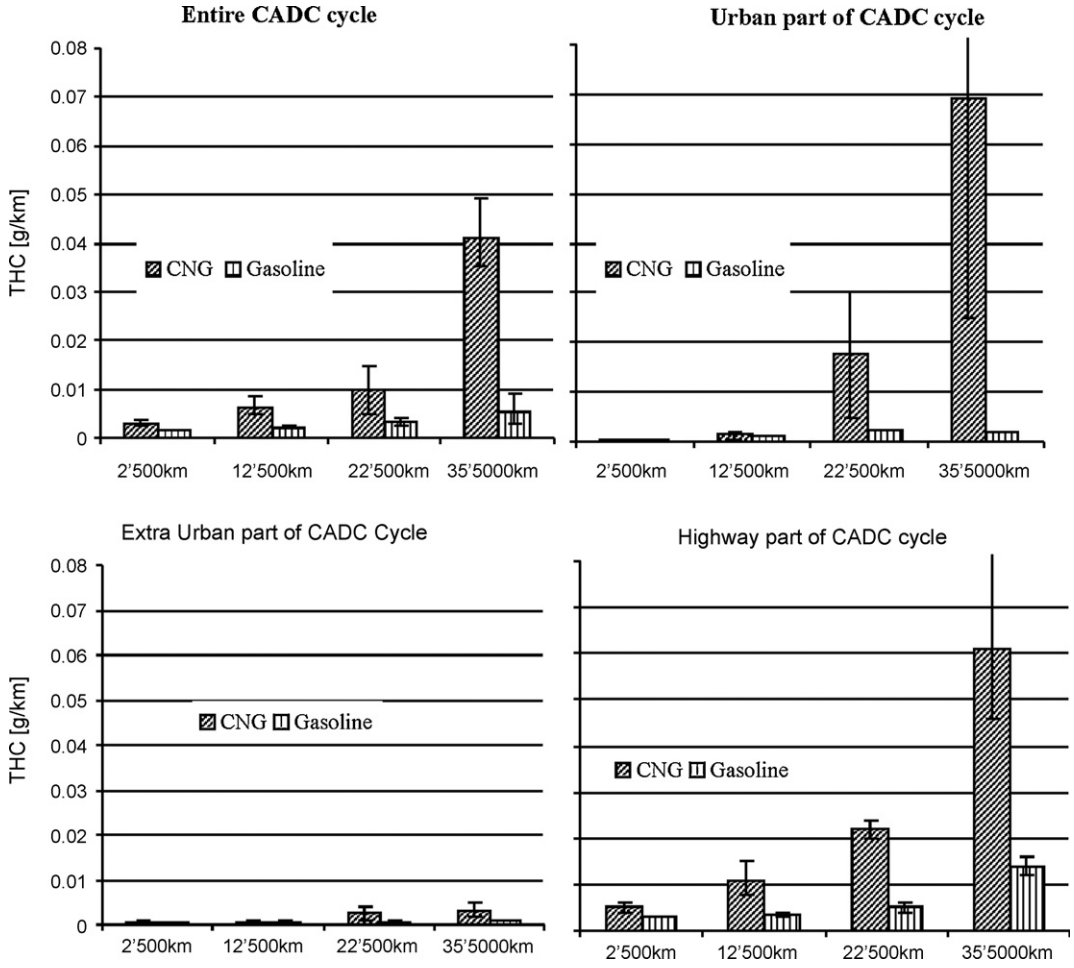

Fig. 3. Averaged tailpipe (downstream of the catalyst) total unburned hydrocarbons over a mileage of 35,000 km during the entire CADC cycle as well as its three consecutive parts. The bars extend from the minimum to the maximum observance (cycles have been repeated at least three times).

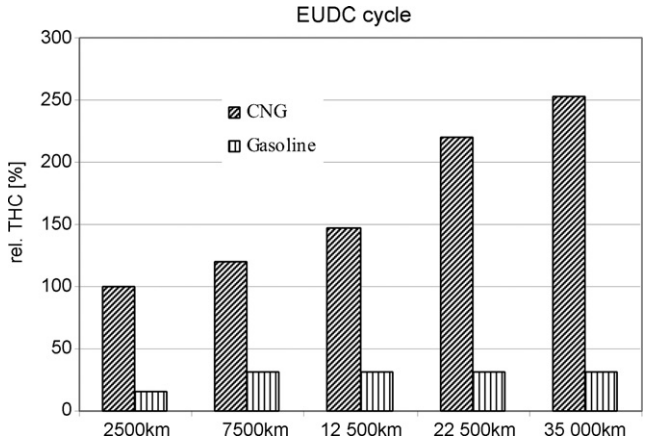

Fig. 4. Relative tailpipe (downstream of the catalyst) total unburned hydrocarbons over a mileage of 35,000 km during the EUDC cycle.

Table 1
Averaged tailpipe (downstream of the catalyst) emissions over a mileage of 35,000 km during the entire CADC cycle

Mileage (km)	THC (g/km)		CO (g/km)		NO_x (g/km)	
	CNG	Gasoline	CNG	Gasoline	CNG	Gasoline
2500	0.003	0.002	0.864	1.839	0.014	0.008
12,500	0.006	0.002	1.457	2.981	0.030	0.011
22,500	0.009	0.003	1.156	3.770	0.013	0.012
35,000	0.041	0.005	1.866	3.246	0.027	0.015

3. Results and discussion

3.1. Catalyst activity

Vehicle emission measurements show a strong increase of the THC tailpipe emission over the relatively short mileage of 35,000 km when the engine is running with CNG fuel. This increase is practically the same regardless of the driving cycle. In Fig. 3, the THC emission is plotted at the CADC driving cycle for selected mileage milestones. The CADC in general was performed three times with CNG and also three times with gasoline at every milestone. Striking is the fact that the identical vehicle, engine and catalysts exhibit only a marginal increase of the THC emissions when operated with gasoline, while the increase with CNG as a fuel is dramatic.

The relative increase of the THC emissions is shown in Fig. 4, in which the THC emissions obtained throughout the EUDC cycle are compared. Once again the rise of the THC emissions during CNG engine operation is extremely high, while very modest during gasoline operation. In Table 1, data is provided concerning the remaining regulated emissions for the CADC. Although the total CO and NO_x emissions at a given mileage vary depending on the fuel used, both CNG and gasoline fuelling results in a doubling of CO and NO_x emissions after 35,000 km (see also Fig. 5). The THC emission also doubles in case of gasoline, whereas for CNG the THC emission is increased by a factor of 8. It is interesting to note that up to 22 500 km the THC emission in case of CNG is tripled, which already hints at a selective and CNG related THC conversion deficiency. Given exhaust temperatures in the catalyst entrance of over 633 K and under 1123 K during the CADC cycle (Fig. 2), as well as the very low deterioration of the performance of the identical catalyst with gasoline fuelling (exhaust temperatures are slightly higher), it is clear that the selective deterioration is neither cold start and light-off nor high temperature sintering effects related.

Fig. 5 shows, next to CO, NO_x and THC, also the NMHC emissions for the entire CADC both for gasoline (left) and CNG (right) after 2500 km and 35,000 km. In case of gasoline the total NMHC emissions are almost identical with the THC emissions, showing that the methane fraction is only minor. When CNG is used as a fuel, the NMHC fraction is practically nil, the THC almost exclusively composes of methane. The CO_2 emissions, not shown in the figure, slightly decreased during the examination period independent of fueling as can be expected due to the reduction of the high friction of the new engine.

3.2. Catalyst characterization

Fig. 6 shows deconvoluted XP-spectra of a new u-TWC (Fig. 6a), a new p-TWC (Fig. 6b) and pure zirconia powder (Fig. 6c), recorded in an energy range between 360 eV BE and 305 eV BE. The ZrO_2 spectrum (Fig. 6c) was used as a basis for peak deconvolution. The Pd signal positions in Fig. 6a and b (Pd $3d_{3/2}$: 342.5 eV BE, Pd $3d_{5/2}$: 337.25 eV BE) hint at palladium primarily in the oxidation state between +IV and +II ($Pd_{Lit.}$ $3d_{5/2}$ (PdO): 336.1–336.6 eV BE [12], $Pd_{Lit.}$ $3d_{5/2}$ (PdO_2): 337.8–338.2 eV BE [12]), whereas the Rh signal position (Fig. 6a, Rh $3d_{3/2}$: 314.25 eV BE, Rh $3d_{5/2}$: 309.5 eV BE), points to an oxidation state of +III or higher ($Rh_{Lit.}$ $3d_{5/2}$ (Rh_2O_3): 308.2–308.8 eV BE [12]). The pronounced Zr $2p_{1/2}$ and Zr $2p_{3/2}$ signals (346.25 eV BE and 332.5 eV BE, respectively) partially overlap with the Pd signals. The platinum concentration was below the XP detection limit. Dashed lines in Fig. 6 can be attributed to satellite signals.

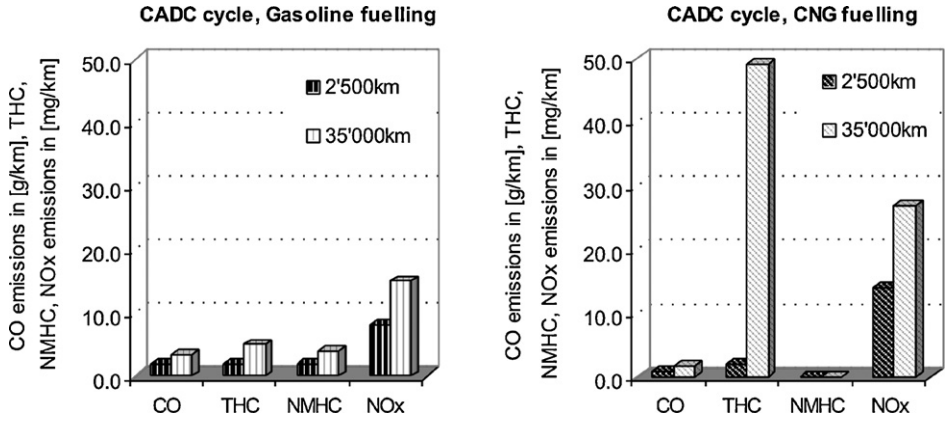

Fig. 5. CO, NO_x, THC and NMHC emissions for the entire CADC both for gasoline (left) and CNG (right) after 2500 km and 35,000 km.

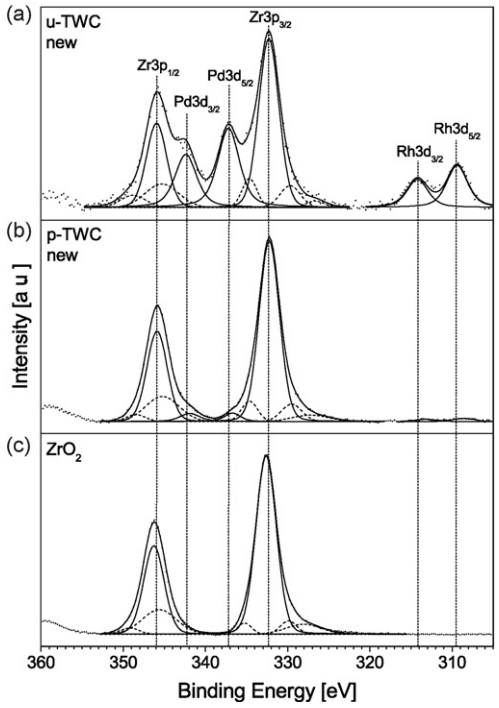

Fig. 6. Deconvoluted XP-spectra of the new u-TWC (a), the new p-TWC (b) and pure ZrO_2 (c) recorded within 360–305 eV BE. All three spectra show Zr 3p signals, Pd 3d and Rh 3d signals are only clearly discernable in case of the new u-TWC (a).

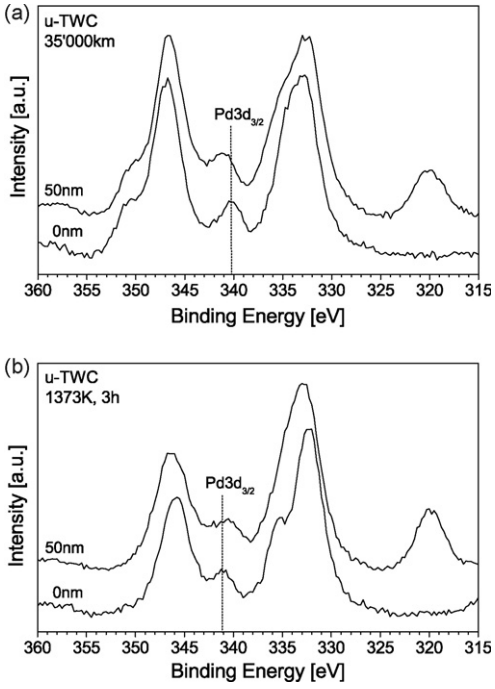

Fig. 8. Pd $3d_{3/2}$ XPS peaks measured before and after sputtering of 50 nm in case of the vehicle aged (a) and 1373 K/3 h oven aged (b) u-TWC. The signal at 320 eV BE appearing after sputtering can be attributed to Ar 2s.

Comparison of the Pd signal positions for the vehicle aged (Fig. 7a), oven aged (Fig. 7b) and new u-TWC (Fig. 7c) shows a clear signal shift from higher to lower binding energy. Whereas the new u-TWC contains palladium oxide, both the oven aging in air (1373 K/3 h) as well as the vehicle aging resulted in the reduction

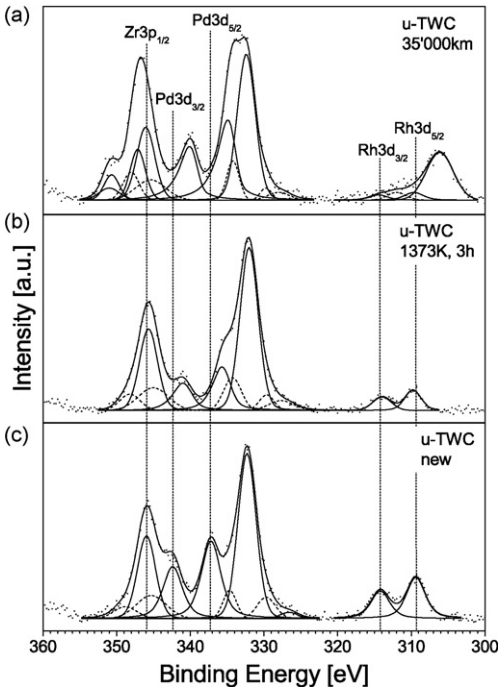

Fig. 7. Deconvoluted XP-spectra of the vehicle aged (a), 1373 K/3 h oven aged (b) and new u-TWC (c), recorded within 360–305 eV BE. The Pd 3d signal positions and relative intensities change with the respective aging procedure.

of Pd (Pd_{oven} $3d_{5/2}$: 335.75 eV BE and $Pd_{vehicle}$ $3d_{5/2}$: 335.0 eV BE; $Pd_{Lit.}$ $3d_{5/2}$ (Pd): 335.1–335.5 eV BE [12]).

Generally, three phenomena would result in the observed signal shift to lower binding energy (Fig. 7a and b). (1) The complete reduction of oxidic to metallic palladium. (2) A very thin PdO film or islands (monolayer range) covering a Pd core. (3) Formation of a thick metallic Pd layer on top of a PdO core. In case of the vehicle aged u-TWC it is shown, that after sputtering (Fig. 8a) the Pd $3d_{3/2}$ signal shifts by about 1 eV to higher binding energy (340.0 eV BE and 341.0 eV BE, respectively). This hints to option (3), meaning that some of the Pd^0 layer is removed during sputtering, thus increasing the signal intensity of the underlying PdO. The formation of the Pd film could be attributed to the alternating rich and lean reaction atmosphere within the u-TWC (λ = 0.98–1.02). During the rich phase palladium oxide could be partially reduced to metallic palladium, whereas during the lean phase the concentration of oxidizing agents might not be high enough to completely reoxidize the metallic Pd film. These results are in agreement with the ones Klingstedt et al. [3] published for the model catalyst system Pd-Ce/Al_2O_3.

In case of the oven aged u-TWC, sputtering does not result in a clear Pd $3d_{3/2}$ signal shift to higher binding energy (Fig. 8b). Instead, the Pd $3d_{3/2}$ signal at 341.0 eV BE has broadened to lower BE and the Pd $3d_{5/2}$ related peak at 335 eV BE can not be resolved any more. In contrast to the vehicle aged TWC, aging in the oven results in modifications according to option (2). With a maximum temperature of 1373 K/3 h, it can be expected that all of the PdO was reduced to Pd, while no complete reoxidation during cooling occurred, resulting in the formation of a thin PdO layer [13,14].

The Pd/Zr and Rh/Zr signal intensity ratios have been calculated from the data presented in Fig. 7 to give an overview of the amount of catalytically active material on the surface. In case of the new u-TWC the Pd/Zr and Rh/Zr ratios amount to 0.23:1 and 0.13:1, respectively. Whereas for the vehicle aged u-TWC the Pd/Zr and Rh/Zr ratios amount to 0.26:1 and 0.03:1, respectively. Especially

Table 2
Specific surface areas according to BET measurements for the new, oven aged, and vehicle aged u- and p-TWCs

Catalyst	Specific surface area (m^2/g)			
	New	1173 K/3 h	1373 K/3 h	35,000 km
u-TWC	43	28	18	23
p-TWC	42	32	18	3

the almost unchanged Pd/Zr ratio (±15% error) is interesting considering the fact that due to thermal effects the vehicle aged u-TWC lost about 50% of its specific surface area (Table 2) and also shows some sintering (compare Fig. 9d and f). The respective ratios for the oven aged u-TWC (Pd/Zr: 0.12:1, Rh/Zr: 0.05:1) are both clearly below the values for the new u-TWC; the SSA of the former being reduced by about 60%. The oven aged u-TWC most likely endured higher temperatures than the vehicle aged u-TWC (maximum temperature reached in a CADC was 1123 K); the reduced

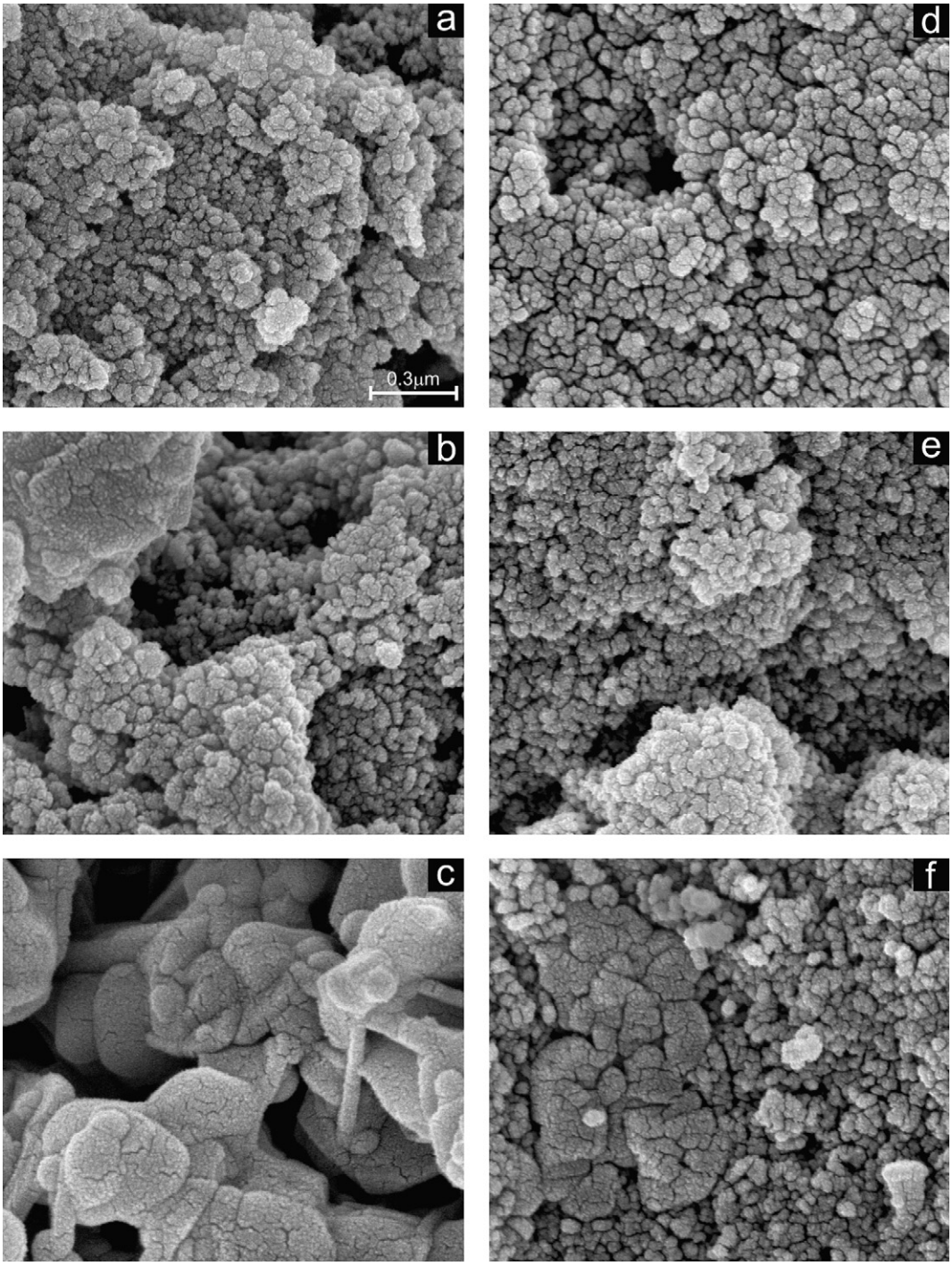

Fig. 9. SEM images of the new (a and d), oven aged at 1373 K/3 h (b and e) and vehicle aged (c and f) p-TWC (left) and u-TWC (right) washcoat surfaces. All images were recorded at ×50,000 magnification.

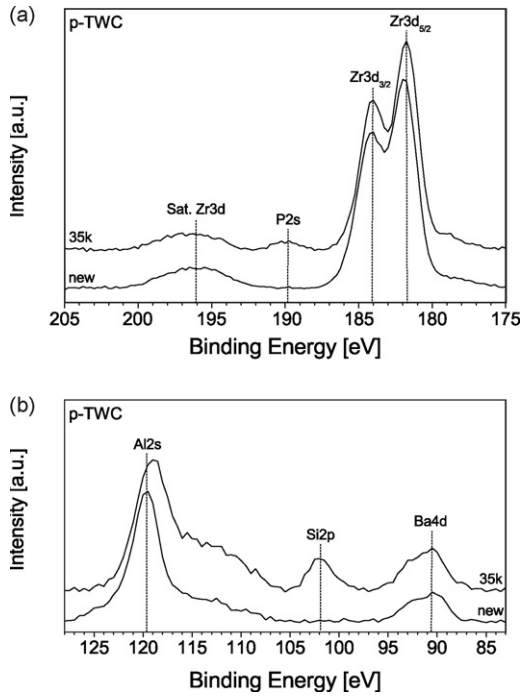

Fig. 10. XP-spectra of the new and vehicle aged p-TWC, recorded within 205–175 eV BE (a) and 128–83 eV BE (b). In case of the vehicle aged p-TWC, P 2s (a) as well as Si 2p (b) signals were detected.

intensity ratios for Pd and Rh can be related to typical thermal induced effects like encapsulation, clustering and diffusion.

Fig. 7a also shows signals related to cationic calcium (Ca $2p_{1/2}$: 351 eV BE, Ca $2p_{3/2}$: 347.5 eV BE; $Ca_{Lit.}$ $2p_{3/2}$ (CaO): 346.2-346.8 eV BE [12]) and magnesium (Mg $KL_{23}L_{23}$ at 306.0 eV BE for AlKα), which are not present in case of the new and oven aged u-TWCs. These contaminants originate from the lubricating oil and were found in even higher concentration on the p-TWC surface. Another lubricating oil based contaminant found was phosphorous (Fig. 10a, 35 k, P 2s at 190 eV BE; $P_{Lit.}$ 2s (phosphates): 190.1–190.9 eV BE [12]). Phosphorous was predominantly found on the p-TWC surface. After sputtering of only 20 nm a P-based XP-signal could not be detected any more. This result is in agreement with the literature [15,16] according to which phosphorous based fouling agents accumulate on the WS surface forming thin phosphate-rich layers or islands. In case of Ca and Mg, no sudden signal intensity loss was detected after sputtering of the first 20 nm. Instead, the signal intensity decreased gradually over the whole depth analyzed (100 nm), including the surface.

Silicon was also detected (Fig. 10b, 35 k, Si 2p at 102 eV BE; $Si_{Lit.}$ 2p (silicates): 102–103 eV BE [12]), on the p-TWC surface in rather large quantities whereas it could not be detected on any of the u-TWC surfaces at all. A potential Si source is the washcoat carrier, consisting of cordierite ($2MgO{\cdot}2Al_2O_3{\cdot}5SiO_2$), a ceramic which is thermally stable up to 1723 K. Although such high temperatures are usually not reached within TWCs, the vehicle aged p-TWC does show signs of excessive thermal stress (95% SSA loss, Table 2; massive sintered surface, compare Fig. 9a and c). Under these extreme thermal conditions diffusion processes from the carrier could have resulted in the accumulation of Si within the WS and on the WS surface. It should be noted that no Si was detected on the oven aged p-TWC. A comparison of the SSA (Table 2) and morphological aspects (Fig. 9b) shows though, that even drastic oven aging conditions (1373 K/3 h) could not induce the amount of thermal damage the vehicle aged p-TWC experienced.

Table 3
RSF (relative sensitivity factor, [12]) corrected Si 2p and Al 2p signal intensities as well as Al:Si signal intensity ratios for the vehicle aged p-TWC as a function of sputter depth

p-TWC	Intensity		Al:Si Ratio
	Si 2p (RSF: 0.283)	Al 2p (RSF: 0.193)	
35,000 km	4791	41,839	8.7:1
20 nm sputtered	2349	44,052	18.8:1
50 nm sputtered	2877	40,181	14.0:1
100 nm sputtered	2374	36,575	15.4:1

Sputtering experiments up to a depth of 100 nm (Table 3, ±15% error) showed that the Si concentration on the p-TWC surface is higher than in the bulk. Within the bulk itself, no concentration gradient was detected, though. Instead, the Si concentration decreased after sputtering of 20 nm and did not significantly change after sputtering up to 100 nm. None of the other analyzed contaminants showed this behaviour. Although Si behaves differently than the other contaminants detected, it cannot be excluded that external sources, other than the lubricating oil, might also be responsible for the Si detected on the p-TWC.

The influence of the described effects on the loss of catalytic activity with regard to methane is difficult to assess. Nevertheless, following conclusions can be drawn from the results presented. The palladium concentrations detected on the vehicle aged and new u-TWC surfaces do not significantly differ. But, in contrast to the new u-TWC, the vehicle aged u-TWC contains PdO particles covered with a layer of metallic Pd. The catalytic oxidation of methane on palladium proceeds via a Mars and van Krevelen mechanism. The first step involves oxidation of methane on PdO and the reduction of the latter, followed by a second step in which Pd is reoxidized to PdO by oxygen [5]. Since the PdO particles in case of the vehicle aged u-TWC are covered with a Pd layer, their catalytic activity for the mechanism described above is most likely limited.

Although the amount of chemical aging compounds (Ca, Mg, P) detected on the u-TWC does not seem to be high, they could have a pronounced deactivating effect on the methane oxidation.

4. Summary and conclusion

Significant THC emission increase was measured over 35,000 km on a bifuel vehicle when operated with CNG. The same vehicle, engine, and catalysts did not exhibit any significant emission deterioration during gasoline operation.

Analysis of the vehicle aged catalysts and comparison to new, unused as well as oven aged counterparts revealed:

- In case of the vehicle aged underfloor catalyst a Pd layer has formed on a PdO core whereas the new u-TWC contained pure palladium oxide.
- Contaminants like P, Ca and Mg, originating from the lubricating oil, were found on both vehicle aged catalysts. Si, not contained in the lubricating oil, was only detected on the pre-catalyst.
- The contaminants showed differing depth distributions.
- The vehicle aged pre-catalyst lost 95% of its original surface area, whereas the underfloor catalyst only lost about 50%.

Given the sensitivity of the catalytic methane oxidation on the palladium states, as stated by the Mars and van Krevelen mechanism, the metallic palladium layer on the outer surface of the vehicle aged catalyst can be identified as the major source for the catalytic activity reduction. In addition lubricating oil components identified on the catalyst surface seem to affect

methane oxidation stronger than the oxidation of higher alkanes. The degree of their contribution to the catalyst aging can only be quantified in future model catalyst experiments.

Acknowledgments

The authors gratefully acknowledge financial support from Novatlantis and the Swiss Federal Office for Energy (SFOE).

References

[1] J. Gieshoff, in: C. Hagelüken, et al. (Eds.), Autoabgaskatalysatoren – 2. Aktualisierte und erweiterte Auflage, Expert Verlag, Renningen, 2005, p. 47.
[2] E.S.J. Lox, B.H. Engler, in: G. Ertl, H. Knözinger, J. Weitkamp (Eds.), Environmental Catalysis, Wiley-VCH, Weinheim, 1999, p. 1.
[3] F. Klingstedt, A.K. Neyestanaki, R. Byggningsbacka, L.-E. Lindfors, M. Lunden, M. Petersson, P. Tengström, T. Ollonqvist, J. Väyrynen, Appl. Catal. A 209 (2001) 301.
[4] C. Bach, C. Lämmle, R. Bill, P. Soltic, D. Dyntar, P. Janner, K. Boulouchos, C. Onder, T. Landenfeld, L. Kercher, O. Seel, J.D. Baronik, SAE Paper 2004-01-0645.
[5] T.V. Choudhary, S. Banerjee, V.R. Choudhary, Appl. Catal. A 234 (2002) 1.
[6] C. Nellen, K. Boulouchos, MTZ 61 (2000) 54.
[7] P. Dimopoulos, C. Rechsteiner, P. Soltic, C. Laemmle, K. Boulouchos, Int. J. Hydrogen Energy, doi:10.1016/j.ijhydene. 2006.12.026, 2007.
[8] A. Takigawa, A. Matsunami, N. Arai, Energy 30 (2005) 461.
[9] European Directive 70/220/EC.
[10] A.M. Vasic, M. Weilenmann, Environ. Sci. Technol. 40 (2006) 149.
[11] XPS International, 754 Leona Lane, Mountain View, California, 94040, USA, E-mail: bvcrist@xpsdata.com, Homepage: www.xpsdata.com.
[12] J.F. Moulder, W.F. Stickle, P.E. Sobol, K.D. Bomben, in: J. Chastian (Ed.), Handbook of X-Ray Photoelectron Spectroscopy, Perkin-Elmer Corporation, Minnesota, 1992
[13] A.K. Neyestanaki, F. Klingstedt, T. Salmi, D.Y. Murzin, Fuel 83 (2004) 395.
[14] R.J. Farrauto, M.C. Hobson, T. Kennely, E.M. Waterman, Appl. Catal. A 81 (1992) 227.
[15] C. Larese, F. Cabello Galisteo, M. Lopez Granados, R. Mariscal, J.L.G. Fierro, M. Furio, R. Fernandez Ruiz, Appl. Catal. B 40 (2003) 305.
[16] M. Lopez Granados, C. Larese, F. Cabello Galisteo, R. Mariscal, J.L.G. Fierro, R. Fernandez-Ruiz, R. Saguino, M. Luna, Catal. Today 107–108 (2005) 77.